Available online at www.sciencedirect.com

ScienceDirect

journal homepage: http://www.elsevier.com/locate/rpor

Original research article

Cardiac risk and MCNP/SISCODES doses in RT of the left internal mammary chain with photon and electron portals

Tarcisio Passos Ribeiro de Campos[1,*], *Bruno M. Mendes*[1,2], *Bruno Trindade*[1], *Wagner L. Araujo*[1]

[1] *Programa de Ciências e Técnicas Nucleares, Departamento de Engenharia Nuclear, Universidade Federal de Minas Gerais, Av. Presidente Antônio Carlos, 6627, EE, Bloco 4, S.2285, CEP: 31270901, Belo Horizonte, MG, Brazil*
[2] *Centro de Desenvolvimento da Tecnologia Nuclear (CDTN/CNEN), Av. Presidente Antônio Carlos, 6.627, CEP 31270-901, Belo Horizonte, MG, Brazil*

ARTICLE INFO

Article history:
Received 13 October 2016
Received in revised form
18 December 2017
Accepted 7 July 2018
Available online 13 August 2018

Keywords:
Internal mammary chain
Breast radiation therapy
Lymph nodes
Electron
Photon

ABSTRACT

Aim: The present study evaluated the increment of cardiac risk (CR) and absorbed dose in radiotherapy of the internal mammary chain (IMC), in particular with photon portals of 4 6 MV, and cobalt therapy (Co60); and, electron portals of 8, 12 and 16 MeV applied in the left breast, considering the adoption of a combined photon (16 Gy) and electron (30 Gy) protocols.
Materials and methods: The modified ICRP-reference female model of 60 kg, 163 cm and 43 years of age, coil RCP-AF, was modelled. The MCNP6/SICODES codes were employed, where the spatial dose distributions and dose-volume histograms were generated. Toxicity limits and a CR model were considered.
Results: CR associated with the 6 MV, 4 MV and Co60 portals increased 41.1; 40.6 and 34.5%, respectively; while, in 8, 12 and 16 MeV portals, they were 5.0, 32.5 and 49.2%, respectively. High anomalous scatter radiation from electron portals was found in the left lung providing an average dose of 3.3–5.0 Gy.
Conclusions: To RCP-AF, the Co60 portal for IMC-RT presented more attractive dose distribution, whose 16 Gy for photon-component produced less CR increase, 5% lower than the other photon portals. Considering electron portals, the smallest CR increase was produced by 8 MeV portal while 12–16 MeV made the risk higher. There is a call for a less hardened energetic spectrum in order to reduce CR; however, holding suitable IMC penetration. A combined Co60/8–12 MeV may bring benefits, reducing CR. The lowest risk was found to 46 Gy electron portals exclusively.

The research project was conducted under the supervision of: Dr. Tarcísio Passos Ribeiro de Campos, Professor of Departamento de Engenharia Nuclear – DEN, Programa de Pós-graduação em Ciências e Técnicas Nucleares, Universidade Federal de Minas Gerais – UFMG, Av. Presidente Antônio Carlos, 6.627, CEP 31270-901, Belo Horizonte – MG, Brazil.

* Corresponding author.
E-mail addresses: tprcampos@yahoo.com.br, tprcampos@pq.cnpq.br (T.P.R.d. Campos), bmm@cdtn.br (B.M. Mendes), bmtrindade@yahoo.com.br (B. Trindade).

https://doi.org/10.1016/j.rpor.2018.07.004

1. Background

After mastectomy or breast-conserving surgery for breast cancer (CA), radiation therapy (RT) in the lymph nodes (RT-LN) of the internal mammary chain (IMC), of the supraclavicular medial and fossa (SCF) and of the axillary chains (AXL) definitely increases the rate of disease free survival (DFS), metastases free survival (MFS) and the overall survival rate (OS) in patients with breast cancer in stage I to III. Three recent randomized clinical trials, identified by: (i) NCIC Clinical Trials Group MA.20, reported by Whelan et al., 2011, in the period of 2000–2007 with 1,832 patients[1]; (ii) EORT22922-10925 (EORT-European Organization for Research and Treatment of Cancer) in 1996–2004 with 4004 patients[2]; and, (iii) reported by Hennequim et al, 2013, coil FR, from 1991 to 1997 with 1334 patients (based on meta-analysis),[3] confirmed these findings. Such findings may point to the RT-LN application in breast CA in stages I–III.

RT-LN including SCF and IMC, in MA20, FR and EORTC studies, resulted in an increase in OS. In summary, the general benefit of RT-LN in OS was 1.6% at 5 years with MA20, 1.6% at 10 years with EORTC and 3.3% at 10 years with FR. RT-LN has also determined a 3% additional time in DFS and MFS.[4,5]

Past and current recommendations to RT-LN with IMC, SCF and AXL portals are still not clear. In the past, Lacour et al., 1983, showed no evidence of prognostic change with RT-IMC complements to breast RT.[6] There was no indication of benefit in RT-IMC in cases with T < 5 cm, unless the tumor was present in the internal or central quadrant (IQ/CQ) with LN+. At that time, no significant benefits were identified in comparison with the risk of cardiac toxicity present in RT-LN in IMC in the case of T in IQ with LN−.[6,7]

Currently, in AXL committed to at least three LN+, it is prudent to irradiate the lymphatic drainage pathways, including SCF portals and IMC.[8] Then, AXL, IMC and SCF portals may be needed when occur lymphatic chains compromised, AX+ with axillary lymphatic complete drain or missing. It is expected that the IMC and SCF portals promote the reduction of loco regional recurrence (RLR).[8–11]

The MA20 studies, FR and EORT brought new important information that confirms the need for RT-LN in patients with 1 to 3 LN+. Poortmans et al., 2015, suggests the reintroduction of RT-LN in IMC with LN+ or when T is medial or central at breast.[2] Reintroduction of RT-LN means the dosimetry and risk reassessment associated with photon beams for megavoltage accelerators or Co60; and, with electron beams, in the light of robust planning tools, such as provided by the Monte Carlo technique, where the reliable anatomical representation, equivalence in mass density and chemical composition of the region under study can be reproduced. Thus, one can have the knowledge of the absorbed dose produced by the direct and scatter radiation in the organs, incorporating the anatomical and morphological heterogeneity of the tissues.

Toxicology Working Group defined a maximum tolerated dose that provides a risk of incidence of a clinical effect in a group of patients at *n* years in a specific organ.[12] The organs with the greatest potential for risks of developing complications in breast RT are the lungs and heart. The main damage in the lungs is acute and chronic pneumonia, and in the heart, pericarditis and pancarditis.[12]

Portals involving the heart lead to an increase in the rate of cardiac ischemia post-radiation. The rate of occurrence of heart disease is proportional to the average absorbed dose in the heart, starting 5 years post-exposure and continuing until 20 years later. Woman irradiated to the left breast has a higher rate of coronary events than the one irradiated to the right breast. There is no risk alteration associated with the size and location of the tumor, or radiation treatment.[13–15]

In agreement with Peres, 2003, T1 and T2 breast CA can receive the IMC portal with doses of 16 Gy of photons complemented with 30 Gy of 12 to 16 MeV electrons, with the aim of reduction of absorbed dose in the lung. In turn, the investigation of the dosimetry of the IMC portal holding 4 MV, 6 MV and Co60, complemented to high energy electrons, becomes relevant considering the possible reintroduction of the RT-LN, whose indications were pointed out in the MA20, FR and EORT studies.[1–3] The Monte Carlo technique coupled with the ICRP/ICRU reference computational phantoms is a robust tool for investigating particle transport especially for dealing with the heterogeneity of the IMC region.

2. Aim

The present study aims to assess the increase in cardiac risk and the absorbed dose distribution provided by the electron and photon portals in IMC, in particularal with 4 and 6 MV megavoltage RT or Co-60, and electron beams of 8, 12 and 16 MeV, applied in the left breast due to the higher proportion of the heart exposure. The dosimetry, based on Monte Carlo, will cover the internal volume of the thorax, head and neck, the primary and scatter radiation, both into and outside the radiation field generated by the electron and photon portals.

3. Methods

3.1. *Computational model*

The ICRP and ICRU provided reference phantoms for masculine and feminine adults.[16,17] The female model, named RCP-AF, represents a woman of 60 kg and 163 cm. The patient whose images raise the phantom was 43 years old. The model had the dimensions of $137 \times 348 \times 299$ voxels of $1.775 \times 4.84 \times 1.775\ mm^3$. The number of tissues was 138 and 53 materials were defined. The chemical composition and density of these materials have been described in the ICRP110.[17] A computational routine made *in-house* was elaborated for rotation and adjustment of the upper limbs of the RCP-AF. This routine was used to hyperextend the phantom left arm to 90 degrees with correction of the anatomy of the axilla.

3.2. *Definitions of clinical structures and IMC field*

The organs at risk (OARs) were the heart-wall, right lung, left lung, left and right breast with glandular breast tissue and fat tissues. The prescribed target volume (PTV) was outlined in the model RCP-AF as a set of voxels in the region occupied by

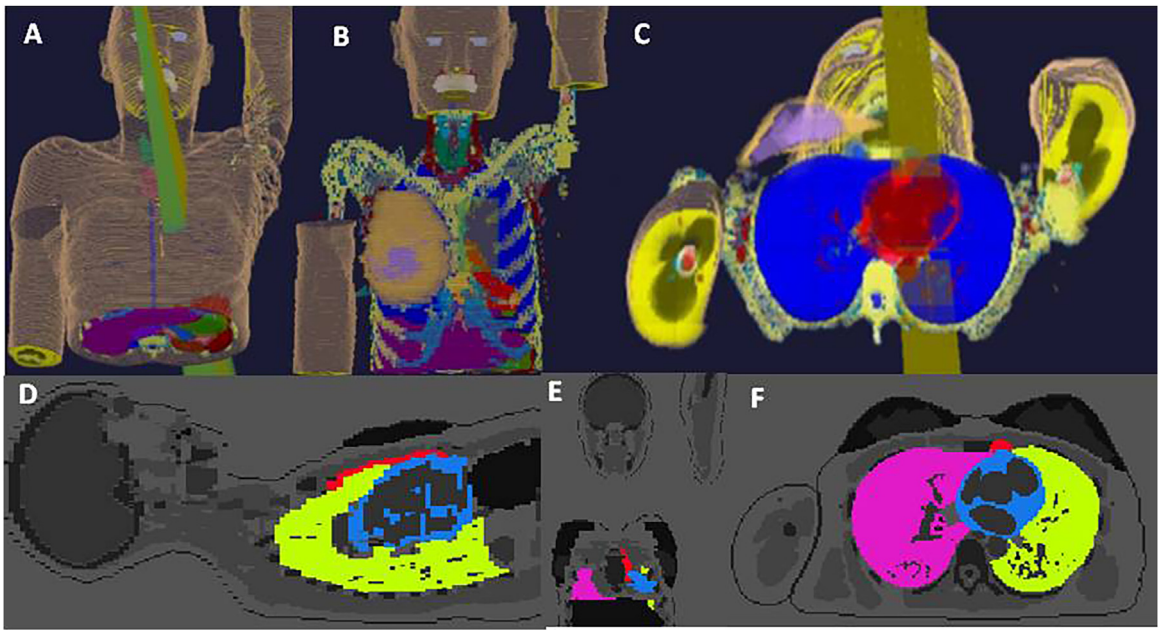

Fig. 1 – Portal description; (A) three-dimensional view of the rectangular field 3.5 × 10 cm in isocenter, (B) the field entry with tissue removal for best viewing; (C) axial section of the model showing the field, isocenter in (3.5;0;9.5), distance source-isocenter 100-cm, unitary weight; rotation of the gantry Yan = −90, Pitch = −100; Roll = 0; (D–F) color representation of the PTV and the OARs as left-lung, right-lung and heart-wall.

the IMC. Both PTV and OARs were presented in Fig. 1. A direct photon/electron field was set to irradiate the IMC, as described in the literature.[8] The field was rotated 10 degrees laterally to protect the spinal cord, as depicted in Fig. 1.

3.3. *Dose and volume constraints*

The restrictive parameters were as follows: TD5/5 of 30 Gy and TD50/5 of 35 Gy to 100-cm^3 of the lung; or, TD5/5 of 15 Gy and TD50/5 of 25 Gy to the whole exposure lung; TD5/5 of 45 Gy and TD50/5 of 55 Gy for pancarditis and pericarditis to 60% of the heart volume; or 70 and 80 Gy, when 25% of the heart is irradiated.

3.4. *Prescribed dose in IMC*

The prescribed dose (D100) for photon fields was 16 Gy, calculated at 3-cm deep in the PTV such that the value of the dose in 95% of the PTV exceeded D100. For electrons, the D100 was 30 Gy, whereas the other parameters followed those from photon portal.[8] The compliance index (IC) was evaluated as the ratio between the target-volume which received doses higher than D100 and the total target-volume. This ensured that 95% of the target-volume received at least D100.

3.5. *Emission source*

The source was simulated with 10^4 unitary vectors distributed in an area representative of a surface bellow the flatness filter in an accelerator gantry. Those vectors were pointed to a rectangular field defined in the isocenter. A randomized variability in the vector direction was assumed to be 0–5 degrees. Each vector received a corresponding weight, which refered to the probability of particle emissions in that direction. The weight matrix was calculated such that the absorbed dose at 10-cm depth in the water box produced a surface profile of absorbed dose in 80% of the effective area of irradiation, with standard deviation less than 3%; thus the flatness of the radiation beam was ensured.

3.6. *Energy spectra of the RT beams of 4, 6 MV, Co60 and electrons*

The main five emission energies of the photons emitted by Co60 are 0.346, 0.826, 1.173, 1.333 and 2.159 MeV with the yields of 7.60×10^{-5}, 7.60×10^{-5}, 1.00, 1.00, 1.11×10^{-5}, respectively. The probabilities of photon emissions were normalized by the total number of particle emission. The 4 MV and 6 MV spectra of the Varian were used in these simulations. The emission spectra of electrons were considered to be monoenergies of 8, 12 and 16 MeV. The same spatial and vetorial source distributions were considered for photons and electrons.

3.7. *Computer codes used in the simulation in RT*

The computer simulation was generated using the SISCODES® and MCNPv6® codes.[18] The output T̈ally F6+:pẅas employed for photons, and T̈ally *F8:eẗo electrons, both with 10^6 particles. For comparison, the absorbed energy data generated for electrons was divided by the mass of the voxel for each tissue, generating absorbed dose in Gy. All statistical tests applied by MCNP® were checked and approved.[13] A set of energy with intervals of 100-keV was considered for studying the continuous spectra of 4 and 6 MV; also, for Co60 discrete spectrum.

The same was adopted for electrons. Variance reduction techniques were not applied. The results were normalized and presented in the absorbed dose rates per unit of particle emitted. Dose ranges were plotted from 10% up to 100% in function of the maximum dose rate (MDR) for high dose analysis; and 1% range between 1-10% of the spatial domain outside the radiation field whose doses were provided with the scattered radiation.

3.8. *Risk assessment of relevant cardiac events*

The model of Darby[13,14] that describes the increase of the risk of the relevant heart effects at the 5 to 30-year post radiation was adopted. It was a linear expression of the risk in function of the average heart dose, with no dose threshold, such as:

$$R = \alpha \times D, \quad (1)$$

where R is the rate of increase in the occurrence of cardiac events (95% confidence interval) and D is the average heart dose in Gy; and α is the coefficient equal to 7.5% Gy^{-1} (confidence interval 95%, 2.9–14.5; $p < 001$).[13]

4. Results

4.1. *Spatial dose distribution into and outside the field of radiation*

One can observe the spatial dose distribution in the chest taken in the Pz76 section in function of the IMC irradiation by all photons and electrons portals (Fig. 2A).

In reference to the Co60, 4 MV and 6 MV portals, it is observed that the differences of the deep doses (15–20 cm) from the three-portals were soft; however, there is a gradual growing of a spread field of the deep spatial dose distribution covering the heart-wall in accord to the hardening of the spectrum from Co60, 4 MV toward 6 MV, respectively. A broad field of the absorbed dose distribution in the internal organs of the female chest was observed in the photon portal.

The spatial absorbed energy distributions in MeV in the thorax, generated by 8, 12 and 16 MeV portals were presented in Fig. 2B, which depicted the PZ76 axial sections of the phantom. One can observe that the 8 MeV portal held lower penetration and had almost not deposited ionizing radiation in the heart-wall. Otherwise, 12 and 16 MeV reached the heart and provided large energy deposition on the whole heart. The energetic electrons can cross the lungs with very low deposition of energy due to the small mass density of the lung tissue (0.22 up to 0.70 g cm^3) that changes with the respira-

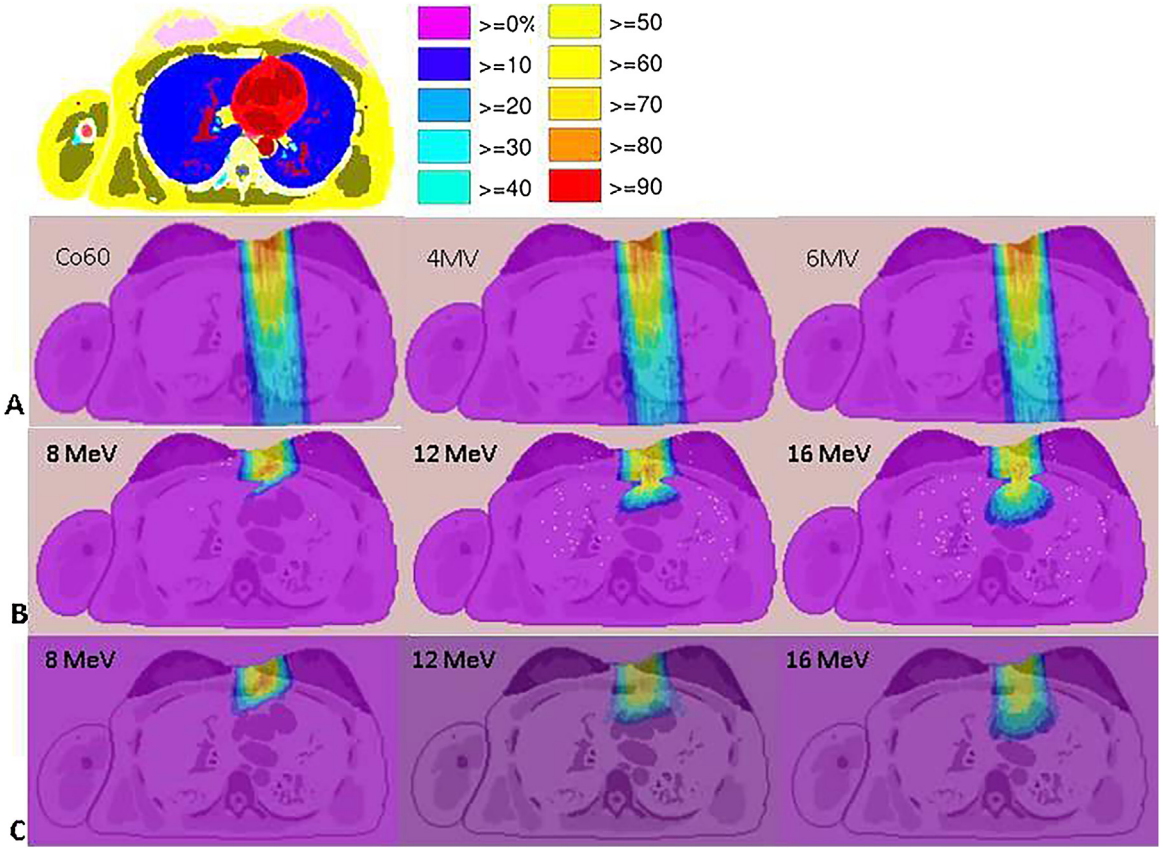

Fig. 2 – Normalized spatial distribution in the axial section at PZ76 to (A) the absorbed dose of the 4 MV, 6 MV and Co60 photons portals; (B) the absorbed dose of the 8, 12 and 16 MeV-portals, and (C) the absorbed energy of the 8, 12 and 16 MeV-portals, in IMC, reproduced in intervals of 100% to 10% in the field of irradiation.

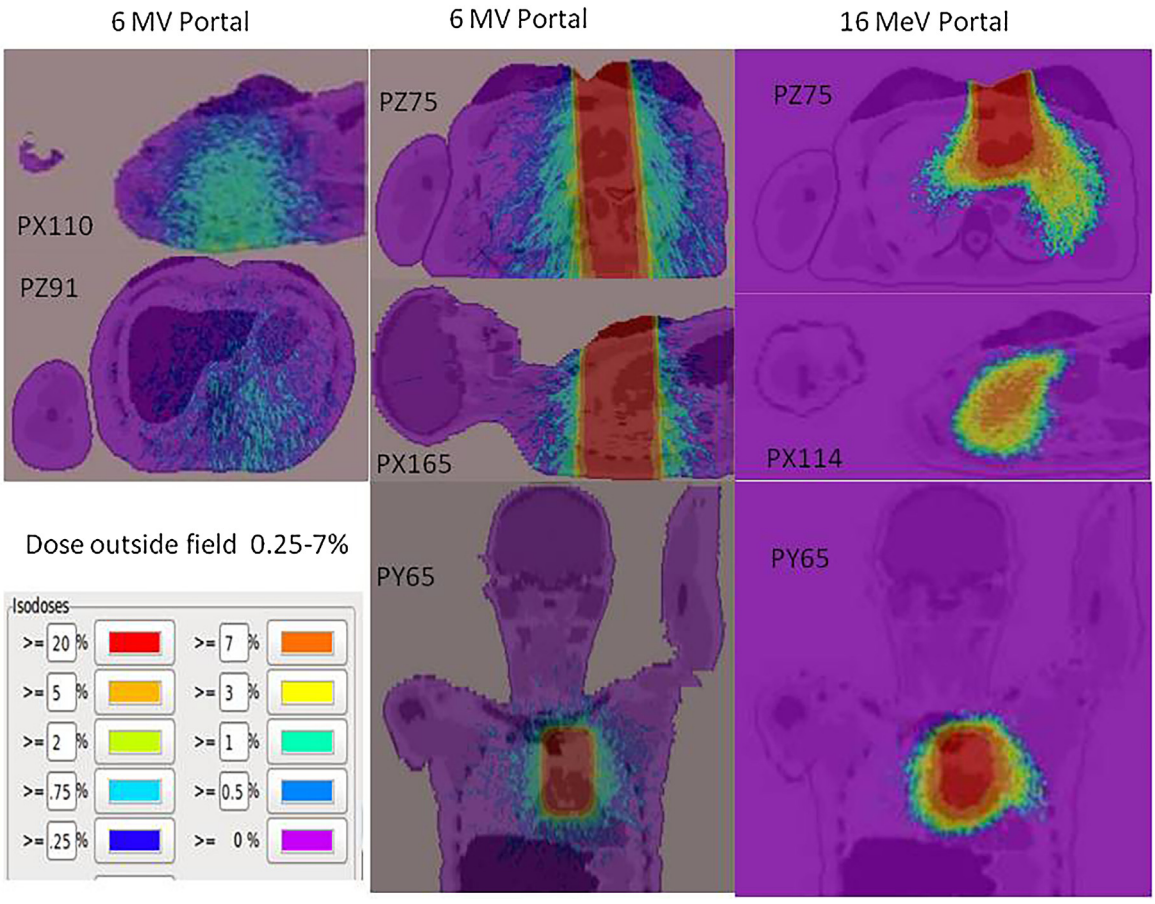

Fig. 3 – Spatial dose distribution in the axial, sagittal and coronal sections of the IMC irradiation with 6 MV-portal, maximum value 0.0015104 MeV g^{-1} p^{-1} (161,25,20), reproduced in intervals of 7% to 0.25% generated by the scattered radiation on the thorax organs.

tory cycle. This fact justified the increase penetration of the 12 and 16 MeV portals crossing the lungs toward the heart-wall. Fig. 2C provides an image of the dose distribution in the same section. Their dose profiles presented continuous distribution while absorbed energy presented very low value in the lungs, generating a discontinued distribution. Indeed, since the lung mass is very low due to small mass density, doses in the lung became equivalent to the dose on the muscle tissue and heart-wall, generating a continuous distribution from the skin to the heart crossing the lungs.

In reference to the Co60, 4 MV and 6 MV portals, a wide range of radiation exposure produced outside the photon portal was observed. The dose distribution outside the field was provided by the scatter radiation which covered a large portion of the internal organs. These expositions represent 0.25% to 7% of the MDR, identified in the entry portal. The spatial dose distributions produced by secondary radiation, outside the geometry of the main field for the 6 MV and 16 MeV portals, were illustrated in Fig. 3 at a set of 2D sections identified by their positions in the model.

The scattered radiation from 8, 12 or 16 MeV-portals out of the field presented a complete different profile in comparison to the scattered radiation from the photon portals. The electron and photon secondary particles scattered from primary electrons at the IMC portals generated doses at 0.25% to 7% of the MDR in the ipsilateral lung, as shown in Fig. 5B for the16 MeV-portal.

4.2. *Dose analysis and histograms in PTV and OARs*

The numbers of particles emitted by the source to produce the D100 of 16 Gy for photons and 30 Gy for electrons were such that the compliance index (IC) exceeded 0.95. The IC values for the 4 MV, 6 MV and Co60 portals were satisfactory, above 0.98; being 0.99 for Co60. And, the numbers of photons required to generate the prescribed dose with IC above 0.95 were 1.38E+14, 1.23E+14 and 1.45E+14, respectively, to the 4 MV portals, 6 MV and Co60. The IC values for 8, 12 and 16 MeV portals were 0.774818, 0.806295, 0.799031; while the numbers of particles needed to reach at least 30 Gy (D100) in PTV were 3.95E+12, 4.09E+12, 4.10E+12, respectively. The IC variations for the electron portals are explained by the variability of the z-depth of the IMC voxels in addition to the irregularity of the skin surface produced for the contours of the breast.

Table 1 provides the average and maximum doses in the heart-wall, pulmonary, glandular and adipose tissues of the right and left breast regarding RT of the lymph nodes into IMC by the 4 MV, 6 MV and Co60; and, by 8, 12 and 16 MeV portals.

The smallest set of minimum, maximum and medium absorbed doses for all organs at risk were reached through the

Table 1 – Maximum and average doses in the organs at risk for 4 MV, 6 MV and Co60 portals and 8, 12 and 16 MeV portals in RT-LN in CMI.

Tissues AF-ICRP110		Dose [Gy] in OARs at D100 of 16 Gy photon and 30 Gy electron at PTV											
		Average						Maximum					
		6 MV	4 MV	Co60	8 MeV	12 MeV	16 MeV	6 MV	4 MV	Co60	8 MeV	12 MeV	16 MeV
L	HW	5.5	5.4	4.6	0.7	4.3	6.6	26.3	25.8	21.2	21.2	29.9	30.6
	LT	2.7	2.6	2.2	0.3	2.1	3.2	25.7	25.5	21.2	25.0	31.3	31.9
	AB	2.9	2.9	2.5	3.3	4.8	5.0	29.7	29.3	24.7	31.1	30.8	31.5
	GB	0.5	0.5	0.5	0.8	0.9	0.9	24.2	23.8	20.1	27.7	28.1	28.6
R	LT	0.3	0.3	0.3	0.3	0.7	0.6	24.1	23.9	21.0	24.9	30.7	30.8
	AB	0.1	0.1	0.1	0.1	0.1	0.1	14.4	14.3	12.4	15.4	16.6	16.7
	GB	0.0	0.0	0.0	0.0	0.0	0.0	0.2	0.2	0.2	0.0	0.0	0.0

HW – heart wall; AB – adipose tissue breast; GB – glandular tissue breast; LT – lung tissue; L – left; R – right.

Co60 portal, justified by the lower radiation beam penetration associated with the lower Co60 energy spectrum. The prospect of risk increase of secondary cancer associated with the Co60 portal can also be observed, since the left breast glandular tissue and the left lung tissue received doses of 0.5 Gy and 2.2 Gy. The maximum doses represented hot spots generated in the MCNP6 simulation following the adopted methodological conditions. The IMC represented by the PTV, reproduced in the model by voxels above the lung and below the ribs, lateral to the sternum, is positioned in a high heterogeneous region in the bone–muscle–lung interfaces, taking deep positions varying from 2.5 up to 3.8 cm. Anomalous scatter radiation from the 12 and 16 MeV electron portals was found in the left lung due to the low density of the lung tissue and the portal geometric position (Fig. 3). High average doses of 3.3–5.0 Gy form 8, 12 and 16 MeV were achieved in this organ.

The dose versus volume histograms for the left and right lungs and the heart-wall, considered as organs at risk, and PTVs are shown in Fig. 4. The heart-wall represented the volume that received the largest average absorbed dose in relation to the lungs. The dose values in function to predefined volumes, measured in the dose-volume histograms, were below the TD5/5 and TD5/50 values reported in literature, having for 6 MV and 16 MeV portals the doses of 11-2(33%) and 4-5(100%) for the lung; and, 11-4(25%) and 4-2(60%), in Gy, in respective percentage volumes.

4.3. *Evaluations of the increase of the risk in the heart*

A considerable increase of the risk of major cardiac events in the period of 5 up to 20 years after RT in IMC by photon and electron portals is shown in Table 2.

It is observed that the risk of cardiac events increased in all the three photon portals. However, the lesser value was found for the Co60 portal due to the lesser average dose in the heart-wall. Co60 provided a soft energy spectrum; thus, low penetration resulting in lesser average dose in the lung and heart.

The increases of cardiac risks were 5%, 32.5% and 49.2% for the 8, 12 and 16 MeV portals (Table 2). The cardiac risk for the 16 MeV portal was superior to the photon portals due to the higher average dose in the heart-wall provided by that spectrum; while, for the 8 and 12 MeV portals, the risk is lower than photon portals.

The coefficients of increases of cardiac risks per unit of Gy were 2.56, 2.53 and 2.15 % Gy^{-1} for the 4, 6 MV and Co60 and 0.17, 1.08 and 1.64 % Gy^{-1} for 8, 12 and 16 MeV portals. The combination of photon-dose from photon portals plus electron dose from electron portals to achieve 46 Gy with lower risk was found in electron portals only.

5. Discussion

Different techniques of breast irradiation in exposing heart-wall provide distinct increases of cardiac morbidity at the long term; however, RT-LN in IMC and SCF take a favorable DFS. Thus, the improvement of the irradiation techniques that result in the lesser cardiac exposure can be the solution to this dilemma. This study addressed combined photon portals of 4, 6 MV or cobaltherapy, and electron portals of 8, 12 or 16 MeV, often used in developing countries. The Volumetric Arc Therapy (VMAT) technique often used in US and Europe was not addressed. VMAT may achieve optimal dosimetry in the OARs, including reduced cardiac risk.

It is well known that radio toxicity increases with the dose and the irradiated volume.[8,18,19] Girald and Cosset, 2003, suggest no application of photon portals and recommend to apply electron only.[20] In turn, Perez et al., 2003, suggest the combination of photon and electrons in IMC.[8] Our findings based on a particular phantom anatomy suggested that high energy electron, such as 16 MeV portal, is not a good choice for IMC irradiation. A combined field of Co-60/8–12 MeV may bring benefits, reducing the cardiac risk. However, the lower risk was found in electron only portals, applying 46 Gy, confirming the Cosset suggestion.[20]

Certainly, the cardiac tolerance depends on the heart irradiated volume and the dose per fraction. The RT-LN benefit has been enough in opposition to the potential damage to the cardiac tissue in patients with low risk of regional recurrence.[8,21] The combined photon and electron dose of 45 Gy to a small portion of the heart can probably be accepted and does not cause significant incidence of complications.[22]

RT-LN in IMC increases the dose in the organs of the thorax, while the average dose in the left lung reached 2.2 up to 2.7 Gy and in the heart 4.6 up to 5.5 Gy measured in the study cases. The increase of the risk generated for the photon exposure of the heart reached the values of 35 up to 41%, in agreement with

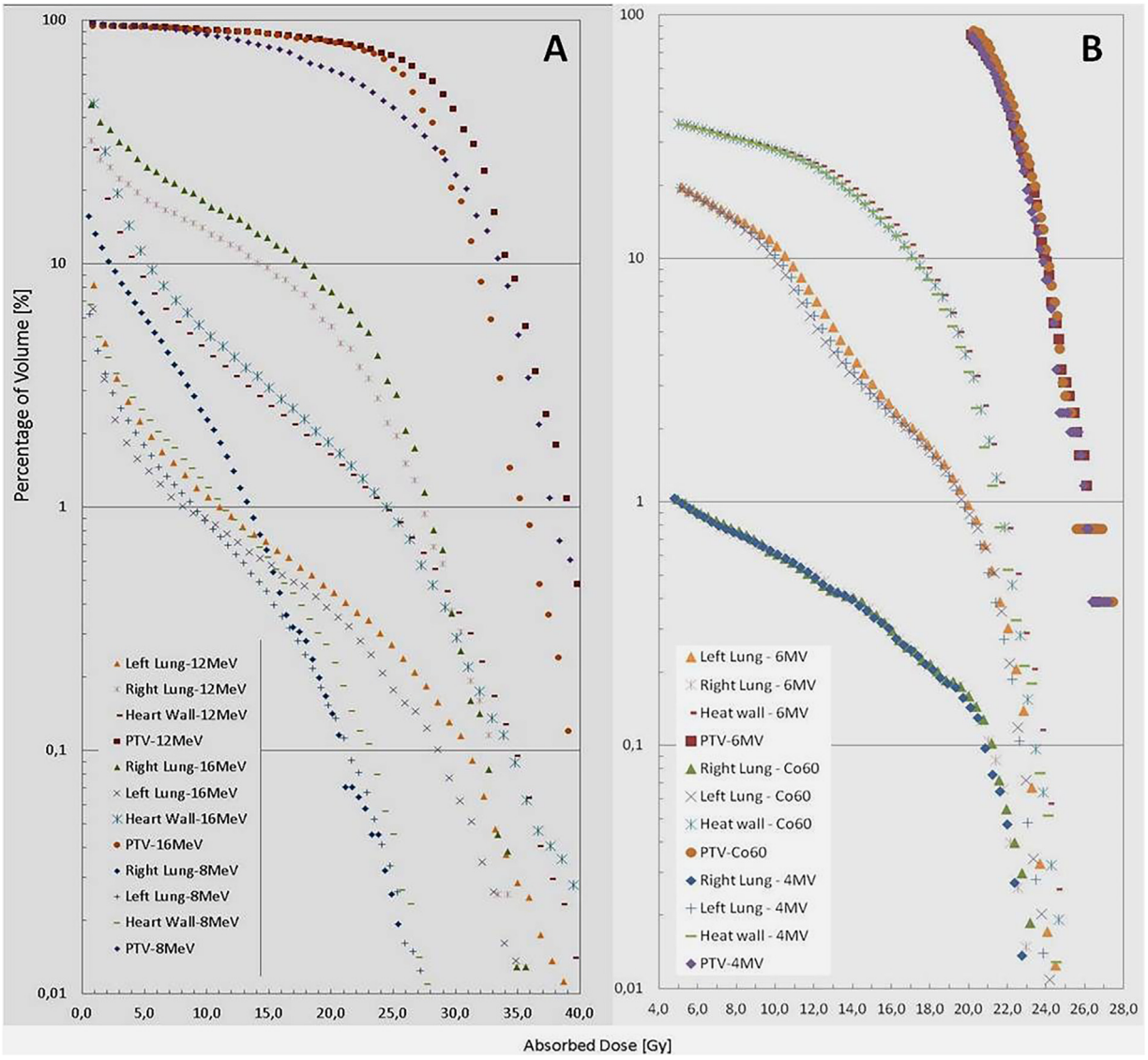

Fig. 4 – Dose versus volume Histogram to (A) the 4 MV, 6 MV and Co60 portals and (B) 8, 12 and 16 MeV-portals for the left-lung, right-lung and heart-wall.

Table 2 – Percentage of the risk increase associated with relevant events in the heart within 5 up to 20 year period. post-RT-LN in IMC in function of the energy spectrum of the 6 MV, 4 MV and Co60 portals and 8, 12 and 16 MeV portals.

Spectra MV	6 MV	4 MV	Co60	8 MeV	12 MeV	16 MeV
Average cardiac dose [Gy]	5.48	5.41	4.60	0.66	4.33	6.56
Increase of risk [%]	41.1	40.6	34.5	5.0	32.5	49.2

the expression proposed by Darby et al.[13,14] Clinical studies conducted over a long term period, more than 10 years, quantifying the induced intra thoracic deleterious effect induced by IMC portal, must be elaborated for better clarifications.

Distinct protocols of breast irradiation, with different geometric fields and spectra, had produced substantially different average doses in the cardiac wall. Possible anatomical variations can also influence the cardiac exposure. Thus, the increase of the risk of deleterious effect in the heart must be studied individually. The present study approached a comparison of the increase in the risk of cardiac deleterious effect, keeping well established conditions of exposure in the same simulator object, with a changeable factor of the spectral variation produced by beams of 4 MV, 6 MV and Co60 and electron beams of 8, 12 and 16 MeV.

6. Conclusions

To RCP-AF, the Co60 portal for RT-LN in IMC presented a more attractive spatial dose distribution, whose dose of 16 Gy for the photon component produced less increase in heart risk, 5% lower than the other photon portals. Considering the electron

portals, the smallest increase in heart risk was produced by the 8 MeV portal while the 12–16 MeV made the risk go higher.

There is a call for a less hardened energetic spectrum of photon and electron components in order to reduce the heart risk; however holding suitable penetration to guarantee prescribed dose on IMC. The combined Co60/8–12 MeV portals may bring benefits, reducing the cardiac risk. Considering the anatomical diversity and density and mass tissue heterogeneities in IMC region, an individualized risk analysis is recommended.

Conflict of interest

Nothing declared.

Financial disclosure

Nothing declared.

Acknowledgements

The research was sponsored by CNPq – Conselho Nacional de Desenvolvimento Científico e Tecnológico (CNPq-REBRAT-SUS). We are grateful to FAPEMIG – Fundacao de Amparo a Pesquisa do Estado de Minas Gerais, due to the postdoctoral fellowship to Wagner Leite Araujo (BPD-00248-14).

REFERENCES

1. Whelan TJ, Olivotto I, Ackerman I, et al. NCIC-CTG MA.20: an intergroup trial of regional nodal irradiation in early breast cancer. Juravinski Cancer Centre at Hamilton Health Sciences, Hamilton, ON. *Can J Clin Oncol, ASCO Annual Meeting Abstracts Part 2* 2011;**29**(18 (suppl)).
2. Poortmans PM, Collette S, Kirkove C, et al. Internal mammary and medial supraclavicular irradiation in breast cancer. *N Engl J Med* 2015;**373**:317–27, http://dx.doi.org/10.1056/NEJMoa1415369.
3. Hennequin C, Bossard N, Servagi-Vernat S, et al. Ten-year survival results of a randomized trial of irradiation of internal mammary nodes after mastectomy. *Int J Radiat Oncol Biol Phys* 2013;**86**:860–6, http://dx.doi.org/10.1016/j.ijrobp.2013.03.021.
4. Budach W, Kammers K, Boelke E, Matuschek C. Adjuvant radiotherapy of regional lymph nodes in breast cancer – a meta-analysis of randomized trials. *Radiat Oncol* 2013;**8**:267.
5. Budach W, Bölke E, Kammers K, Gerber PA, Nestle-Krämling C, Matuschek C. Adjuvant radiation therapy of regional lymph nodes in breast cancer – a meta-analysis of randomized trials – an update. *Radiat Oncol* 2015;**10**:258, http://dx.doi.org/10.1186/s13014-015-0568-4.
6. Lacour J, Lê M, Caceres E, et al. Radical mastectomy versus radical mastectomy plus internal mammary dissection. Ten year results of an international cooperative trial in breast cancer. *Cancer* 1983;**51**:1941–3.
7. Veronesi U, Cascinelli N, Bufalino R. Risk of internal mammary lymph-node metastases and its relevance on prognosis of breast cancer patients. *Ann Surg* 1983;**198**:681–4.
8. Perez CA, Brady LW. *Principles and practice of radiation oncology*. 3rd ed. Philadelphia, United States: Lippincott Williams and Wilkins Publisher; 2003, 2241p.
9. Bellon JR, Wong JS, MacDonald SM, Ho AY. *Radiation therapy techniques and treatment planning for breast cancer (practical guides in radiation oncology*. 1st ed; 2016, 158p.
10. Ludwig MS, McNeese MD, Buchholz TA, Perkins GH, Strom EA. The lateral decubitus breast boost: description, rationale, and efficacy. *Int J Radiat Oncol Biol Phys* 2010.
11. Frank SJ, McNeese MD, Strom EA, et al. Advances in radiation treatments of breast cancer. *Clin Breast Cancer* 2004;**4**(6):401–6.
12. Marks LB, Yorke ED, Jackson A, et al. Use of normal tissue complication probability models in the clinic. *Int J Radiat Oncol Biol Phys* 2010;**76**(Suppl 3):S10–9, http://dx.doi.org/10.1016/j.ijrobp.2009.07.1754.
13. Darby SC, Ewertz M, McGale P, et al. Risk of ischemic heart disease in women after radiotherapy for breast cancer. *N Engl J Med* 2013;**368**:987–98, http://dx.doi.org/10.1056/NEJMoa1209825.
14. Darby SC, McGale P, Taylor CW, Peto R. Long-term mortality from heart disease and lung cancer after radiotherapy for early breast cancer: prospective cohort study of about 300,000 women in US SEER cancer registries. *Lancet Oncol* 2005;**6**:557–65, http://dx.doi.org/10.1016/S1470-2045(05)70251-5.
15. Lara TRM, Fleury E, Mashouf S, et al. Measurement of mean cardiac dose for various breast irradiation techniques and corresponding risk of major cardiovascular event. *Front Oncol* 2014;**22**, http://dx.doi.org/10.3389/fonc.2014.00284.
16. Menzel HG, Clement C, DeLuca P. ICRU, Joint ICRP/ICRU Publication on Adult Reference Computational Phantoms (ICRP Publication 110), Editorial. REALISTIC REFERENCE PHANTOMS: AN ICRP/ICRU JOINT EFFORT, ICRP Publication 110. *Ann ICRP* 2009;**39**(2):1–164, http://dx.doi.org/10.1016/j.icrp.2009.09.001.
17. ICRP. Adult Reference Computational Phantoms. ICRP Publication 110. *Ann ICRP* 2009;**39**(2).
18. Trindade BM, Campos TPR. Sistema computacional para dosimetria de nêutrons e fótons baseado em métodos estocásticos aplicados a radioterapia e radiologia. *Radiol Bras, Abr* 2011;**44**(2):109–16. ISSN 0100-3984.
19. Harris J. Postmastectomy radiotherapy. In: Harris JR, et al., editors. *Breast diseases*. Philadelphia: J.B. Lippincott Co.; 1991. p. 373–87.
20. Giraud P, Cosset JM. Radiation toxicity to the heart: physiopathology and clinical data. *Bull Cancer* 2004;**91**(Suppl 3):147–53. Review. French.
21. Arriagada R. Long term effect of intemal mammary chain treatment. Results of a multivariate analysis of 1195 patients with operabIe breast cancer and positive axillary nodes. *Radiother Oncol* 1988;(11):213–22.
22. Veronesi U, Cascinelli N, Bufalino R. Risk of internal mammary lymph-node metastases and its relevance on prognosis of breast cancer patients. *Ann Surg* 1983;**198**:681–4.